Available online at www.sciencedirect.com
ScienceDirect
Nuclear Instruments and Methods in Physics Research A 582 (2007) 381–389
NUCLEAR INSTRUMENTS & METHODS IN PHYSICS RESEARCH Section A
www.elsevier.com/locate/nima

Measurement of ultra-low potassium contaminations with Accelerator Mass Spectrometry

K.J. Dong[a,b], H.T. Wong[b,*], M. He[a], S. Jiang[a], J.Z. Qiu[a,c], Y.J. Guan[a,d], S.Y. Wu[a], J. Yuan[a]

[a]*Department of Nuclear Physics, China Institute of Atomic Energy, Beijing 102413, China*
[b]*Institute of Physics, Academia Sinica, Taipei 11529, Taiwan*
[c]*Armed Police Force Academy, Langfang 065000, China*
[d]*Department of Physics, Guanxi University, Nanning 530004, China*

Received 30 April 2007; received in revised form 6 August 2007; accepted 29 August 2007
Available online 7 September 2007

Abstract

Levels of trace radiopurity in active detector materials is a subject of major concern in low-background experiments. Among the radioisotopes, ^{40}K is one of the most abundant and yet whose signatures are difficult to reject. Procedures were devised to measure trace potassium concentrations in the inorganic salt CsI as well as in organic liquid scintillator (LS) with Accelerator Mass Spectrometry (AMS), giving, respectively, the ^{40}K-contamination levels of $\sim 10^{-10}$ and $\sim 10^{-13}$ g/g. Measurement flexibilities and sensitivities are improved over conventional methods. The projected limiting sensitivities if no excess of potassium signals had been observed over background are 5×10^{-14} and 3×10^{-17} g/g for the CsI and LS, respectively. Studies of the LS samples indicate that the radioactive contaminations come mainly in the dye solutes, while the base solvents are orders of magnitude cleaner. This work demonstrates the possibilities of measuring naturally occurring isotopes with the AMS techniques.

PACS: 07.75.+h; 92.20.Td; 41.75.−i

Keywords: Mass spectrometers; Radioactivity; Charged-particle beams

1. Introduction

Accelerator Mass Spectrometry (AMS) [1] is an established technique for the detection and measurement of trace level of long-lived radionuclides [2] such as ^{14}C, ^{10}Be, ^{36}Cl. It improves over conventional techniques such as neutron activation analysis (NAA), inductively coupled plasma mass spectrometry (ICP-MS) as well as secondary ion mass spectrometry (SIMS), and has been successfully applied to a wide variety of disciplines like archeology, geology, environmental science, biomedicine, safeguards of nuclear materials and so on [3]. Comprehensive reviews on the merits and constraints on the various techniques can be found in Refs. [4,5].

Measurement of ultra-low concentrations of naturally occurring, as well as cosmic-ray or fission induced radioactive isotopes is an important ingredient of low-count-rate experiments, like those on reactor and solar neutrinos, double beta decays and dark matter searches [6]. Emissions of (α, β, γ) in radioactive decays can produce signatures which mimic and obscure the rare signal events. In order to minimize these isotopes in the detector components, techniques which are flexible, comprehensive and efficient to measure their contaminations with high sensitivities are therefore very crucial.

The TEXONO Collaboration is pursuing a research program in low energy neutrino and astroparticle physics [7]. An important aspect is to devise procedures for measuring such trace radiopurity using the AMS techniques. Significant improvements in sensitivities and flexibilities over existing methods can be expected. Results were published already for the measurement of trace ^{129}I [8] in

*Corresponding author. Tel.: +886 2 2789 6789; fax: +886 2 2788 9828.
E-mail address: htwong@phys.sinica.edu.tw (H.T. Wong).

0168-9002/$ - see front matter © 2007 Elsevier B.V. All rights reserved.
doi:10.1016/j.nima.2007.08.242

Table 1
Comparisons of the various techniques where dedicated research programs were pursued on the measurements of ultra-low potassium concentrations

Technique	Reference	Sample size	Sample type	[^{40}K/sample] (g/g)
HPGe	[12]	~1 kg	No constraints	$<10^{-10}$[a]
ICP-MS	[5]	~1 g	Aqueous solutions water	$<10^{-10}$[a]
	[9]	~100 g		$<10^{-15}$[b]
CTF	[13]	4 ton	Only LS	$<10^{-15}$[b]
NAA	[14]	202 g	No constraints	$<4\times10^{-16}$[b]
	[15]	353 g	No constraints	$<2\times10^{-15}$[b]
AMS	This work	86.5 g	No constraints	$\sim10^{-13}$ (LS)[c]
				$\sim10^{-15}$ (PC)[c]
				$<3\times10^{-17}$[d]

[a]Typical sensitivities with commercially available samples.
[b]Custom-prepared ultra-pure liquid scintillator or water samples.
[c]Commercially produced liquid scintillator (LS) and pseudocumene (PC) samples.
[d]Projected limit if no ^{39}K signals are observed.

inorganic crystal and organic liquid scintillator (LS). The isotope ^{129}I is a long-lived fission fragment, where the corresponding AMS procedures are already matured and well-established. In this article, we report on our efforts and results on potassium (^{39}K). The isotope ^{39}K is stable and exists in large abundance in nature—and there are no prior attempts to measure trace abundance of it with AMS. This poses new experimental challenges and the results reported here represent advances in the field.

Potassium has three naturally occurring isotopes: ^{39}K, ^{40}K and ^{41}K with isotopic abundances of 93.26%, 0.0117% and 6.73%, respectively. Among these, ^{39}K and ^{41}K are stable while ^{40}K has a half-life of 1.248×10^{9} years, where the dominant decay channels are:

$$^{40}\mathrm{K}\rightarrow{}^{40}\mathrm{Ca}+e^{-}+\bar{\nu}_e \quad (\mathrm{BR}=89\%;\ Q_{\beta^-}=1.31\,\mathrm{MeV}) \tag{1}$$

and

$$^{40}\mathrm{K}+e^{-}\rightarrow{}^{40}\mathrm{Ar}^{*}+\nu_e \quad (BR=11\%;Q_{EC}=1.51\,\mathrm{MeV})$$
$$^{40}\mathrm{Ar}^{*}\rightarrow{}^{40}\mathrm{Ar}+\gamma \quad (E_\gamma=1.461\,\mathrm{MeV}). \tag{2}$$

Both decays pose severe background problems to low-count-rate experiments where the signals are at the sub-MeV energy range, such as the studies of proton-fusion (pp) and ^{7}Be solar neutrinos, the searches of cold dark matter, as well as of neutrino magnetic moments with reactor neutrinos [6]. Potassium contaminations in the active detector materials will give rise to a continuous β-decay background up to 1.31 MeV, while those in the passive materials in the vicinity of the detector will produce γ-rays at 1.46 MeV which, after Compton scatterings, can lead to background at the sub-MeV range. The suppression and an efficient measurement technique of ultra-low amount of potassium in a wide spectrum of materials are therefore an issue of crucial significance. As an illustrative example, in order for the BOREXINO [9] and KamLAND [10] experiments to achieve the goals of studying the low energy ^{7}Be solar neutrinos with LS, the required contaminations of ^{40}K should be less than 10^{-18} g/g.

While the radioactive isotope of interest to low-background experiments is ^{40}K, the AMS techniques devised in this work are for the measurement of ^{39}K. The ^{39}K-to-^{40}K ratio of 7971:1 has been demonstrated to be constant [11] for naturally occurring materials, at a level adequate to the ~10% accuracy range relevant to the present measurements. Therefore, a measurement of the stable and most-abundant ^{39}K-contaminations is equivalent to one on the level of ultra-low ^{40}K radio-purities, but with a sensitivity enhancement factor of almost 10^{4}. Furthermore, ^{40}K measurements by the AMS techniques are vulnerable to background contaminations by ^{40}Ca, a stable isotope which exists in abundance in nature. On the other hand, ^{39}K is the only stable isotope for $A=39$, such that isobaric background is greatly suppressed for ^{39}K in mass spectrometry.

The sensitivities of the various techniques where dedicated research programs were pursued on the measurement of ultra-low ^{40}K contaminations are shown in Table 1. Photon counting of the 1.461 MeV γ-line by high-purity germanium (HPGe) detectors [12] is limited by the ambient background. Conventional mass spectrometry techniques [5] like ICP-MS require the samples to be in aqueous solution. This limits the sensitivities on potassium which is naturally occurring and whose salts have high solubility in water. Special dedicated treatment [9] on water purification and sample preparation are therefore necessary to achieve the $\sim10^{-15}$ g/g sensitivity level. In addition, the high plasma temperature and high gas pressure in ICP-MS favor plasma reactions which can lead to a variety of molecular background. The Counting Test Facility (CTF) [13] at the Gran Sasso Laboratory is a 4 ton LS detector which is also the sample to be probed. It took ~30 days to measure only one single sample of LS, and is therefore of limited flexibilities. The NAA techniques for ultra-pure potassium concentrations were recently developed [14,15], where the sensitivities of 10^{-15}–10^{-16} g/g were achieved.

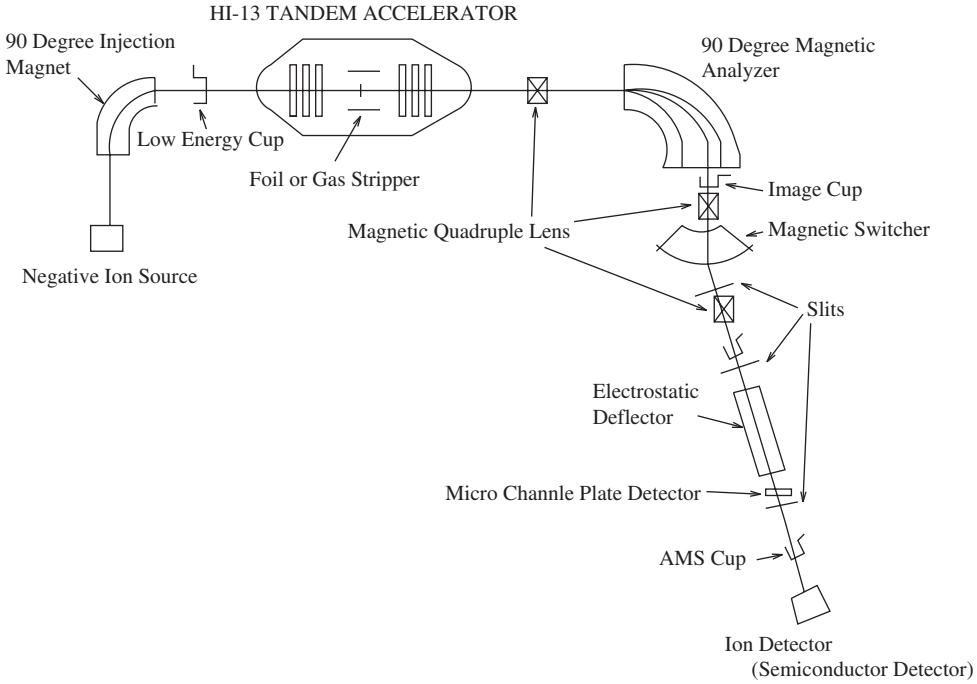

Fig. 1. Schematic layout of the 13 MV Tandem Accelerator Facility at CIAE when it is optimized for AMS applications.

Nevertheless, they still require either special reactor facility [14] or sample preparation techniques [15].

We present the procedures and results on a complementary approach using the AMS techniques in this paper. This approach was adopted because of its promises on sensitivities and versatilities. An organic liquid and an inorganic salt were selected for studies. Once the procedures are established, different batches of samples, each requiring little mass, can be measured in relatively short time. The techniques developed can be easily adapted to other isotopes in trace concentrations, and with different carrier materials.

In a broader context, the studies represent also the direction of extending the frontiers of the AMS techniques to include stable and naturally occurring isotopes, complementary to the research efforts by other groups working on precious metals in minerals [16] as well as various impurities in semiconductors [17]. The AMS detection limits for stable isotopes are in general of the range of 10^{-12}, due to the difficulties of establishing an ultra-clean condition in an accelerator environment. The techniques of background suppression are being intensely pursued by the communities working on low-background experiments. Future advances in these domains may also lead to improvement in the AMS sensitivities on the naturally occurring isotopes.

2. Experimental set-up and procedures

The investigations reported in this article were conducted at the 13 MV Tandem Accelerator Facility China Institute of Atomic Energy (CIAE) [18]. The optimized configuration for AMS applications is shown schematically in Fig. 1.

An organic liquid and an inorganic salt were selected for studies—both being commonly used active detector materials. The choice of a liquid and a solid also requires different experimental procedures to be devised and different systematic effects to be considered. The organic liquid adopted is the standard LS mixture—the dye PPO [2,5-diphenyloxazole] in powder form dissolving in the organic solvent pseudocumene (PC) [1,3,5-trimethylbenzene].[1] The inorganic salt selected was CsI powder,[2] since CsI(Tl) crystal scintillators are being used in reactor neutrino [19] and dark matter [20] experiments. The processing and measurement procedures are expected to be similar with other organic solvent and dyes or inorganic salts.

2.1. Pre-processing

No chemical procedures are necessary for the CsI powder which was directly used in the AMS measurement. However, CsI is a hygroscopic material which can easily deteriorate the vacuum and trigger injector magnet excursion. Accordingly, the CsI samples were deposited quickly on to a cathode of electrolytic aluminium in a clean dry box. The cathode was then baked in an oven at 100 °C for 2 days prior to the measurement.

The LS pre-processing procedures were adapted from those of Ref. [15]. Different LS samples were prepared with

[1]Supplier: Gaonengkedi Science & Technology Co. Ltd., China.
[2]Supplier: Chemtall GMBH, Germany.

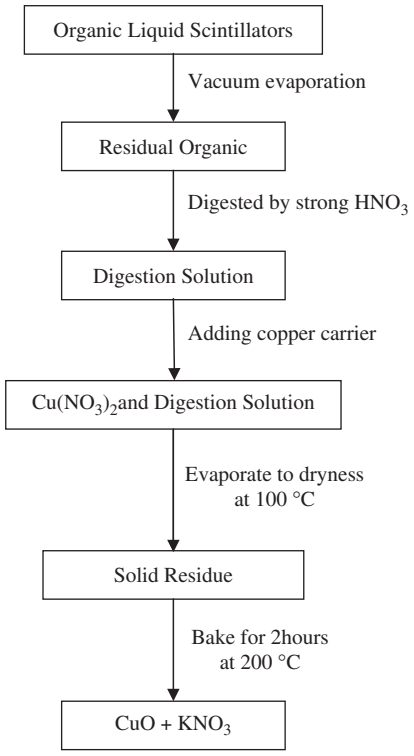

Fig. 2. The flow chart of samples preparation for organic liquid scintillator.

different concentrations of PPO dissolved in pure PC. The procedures are summarized by the flow chart of Fig. 2. All steps were carried out in clean rooms better than the Class-100 grade. Polypropylene bottles were etched in ultra-pure nitric acid[3] and ultra-pure hydrochloric acid over 5 days. The bottles were then rinsed with ultra-pure water and then pure PC, before left to be dried. The LS samples were stored into these bottles for further processing.

Quartz crucibles were etched with 65% ultra-pure hydrochloric acid and 65% ultra-pure nitric acid over a period of one week at sub-boiling temperature. Then they were rinsed with 65% ultra-pure nitric acid and dried at sub-boiling temperature. The LS samples were emptied to the crucibles and evaporated under a vacuum of about 20 Torr. The solid residual left behind was mostly PPO powder, the least volatile component. The mass of solid residuals after evaporation is typically less than 1% of the LS samples. Strong nitric acid was subsequently added to extract the trace elements from the residuals. The acid was heated to 80°C on a hot plate. At this temperature, the PPO samples fully dissolved into the acid, forming a transparent yellow solution where the potassium ions entered the acid phase. Ultra-pure copper[4] with specified potassium concentrations of less than 10 ppb was dissolved into the acid solution. The $Cu(NO_3)_2$ solution was evaporated slowly at 100°C. The residual solid was further baked at 200°C for 2 h. The final substance was mostly CuO, while the trace amounts of potassium existed as KNO_3. These residual solid samples were used as target materials and measured by AMS directly. Only a few volatile potassium compounds exist, such that good recovery of the potassium contaminations from the original LS samples can be expected. This is demonstrated by measurements with different PPO concentrations, to be discussed in detail in Section 3.3.3.

2.2. Injector, accelerator and detector

The ^{39}K concentration in the CsI powder and in the LS were measured with CIAE-AMS facility depicted schematically in Fig. 1. A "multi-cathode source of negative ions by cesium sputtering"[5] was used as the negative ion source. The ions were extracted by sputtering of $^{133}Cs^+$ ions on the sample surface, with an extraction voltage of 20 kV. Forty samples were positioned on the target wheel at one time. The wheel could be rotated without affecting the vacuum conditions such that stable operating configurations were maintained during measurements of a group of samples. For normalizations, the intensities of the $^{127}I^-$ and $^{63}Cu^-$ ions extracted from the samples were measured by the Low Energy Faraday Cup (LECup). These species represent the dominant components of the CsI and $Cu(NO_3)$ target materials, respectively, to which the ^{39}K concentration levels are compared.

The sensitivities of magnetic spectrometry depend on the bending of the charged particles which varies as the square root of a mass–energy–product given by

$$\mathrm{MEP} = \frac{M \cdot T}{Q^2} \tag{3}$$

where M, T and Q are, respectively, the mass, kinetic energy and charge of the particles.

The extracted $^{39}K^-$ ions were focused by a trim einzel lens and a double focusing 90°deflecting magnet where the negative ion beams of interest were selected by their $\sqrt{\mathrm{MEP}}$. The ions were guided to an aperture of 2 mm diameter located at the entrance of the pre-acceleration tube, where they were accelerated up to about 120 keV kinetic energy. The kinetic energy of the ions were further boost to 67 MeV by the main accelerator at a terminal voltage of 7.8 MV. A carbon foil was attached at the head of accelerator. The molecular background was eliminated due to break-up of molecular ions.

After passing through the accelerator tank, ^{39}K ions with charged state 8^+ were selected by a 90° double focusing analyzing magnet with an MEP~200 to suppress the isotopic background. A high-resolution electrostatic deflector was placed at a branch beam line to further reduce the isotopic background and other undesired beam components. The $^{39}K^{8+}$-ions which survived all selections

[3]Supplier of ultra-pure acids: Beijing Chemical Reagent Research Institute, China.

[4]Supplier: Alfa Aesar, USA.

[5]Producer: National Electrostatic Corp., USA; Information: ⟨www.pelletron.com/negion.htm⟩.

were detected by a gold–silicon surface barrier detector which functioned as a counter. The ^{39}K count rates as a function of time were recorded for subsequent analysis.

2.3. Optimizations of operation parameters

The tuning and optimizations of the accelerator parameters were achieved using a similar isotope ^{37}Cl. This avoids contaminations to the subsequent ^{39}K measurements.

Two steps were involved: (1) Negative ^{37}Cl ions from AgCl were emitted from the source and were accelerated by the default terminal voltage of 7.8 MV. All the electrostatic components were optimized to maximize transmission of the ion beam. (2) The magnets were then optimized at the same MEP-values as the subsequent ^{39}K measurements. Accordingly, the kinetic energy T for the $^{37}Cl^-$ was boosted by a higher terminal voltage of 8.22 MV ($=7.8\,\text{MV}\times[M(^{39}\text{K})/M(^{37}\text{Cl})]$). Charge states of $^{37}Cl^{8+}$ were selected. The beam currents measured at the various stages are displayed in Table 2, from which the transmission efficiencies can be evaluated

At the subsequent potassium measurements where $^{39}K^-$ ions were extracted, the strength of the injection magnet [$B(^{39}K^-)$] was set accordingly to

$$B(^{39}\text{K}^-) = B(^{37}\text{Cl}^-) \times \sqrt{\frac{M(^{39}\text{K})}{M(^{37}\text{Cl})}} \tag{4}$$

where B($^{37}Cl^-$) is the B-field optimized with the ^{37}Cl measurements.

3. Measurements and results

Typical data taking of a certain sample consisted of 16 sequential measurements each lasting 100 s, as depicted in Fig. 3 for the ^{39}K-rates in some selected samples. Steady state was reached after several hundred seconds for the ^{39}K-rates, while the beam currents I_{LE} for either $^{127}I^-$ or $^{63}Cu^-$ were stable throughout to better than 10%.

The raw data for each configuration include the mean and variance of the ^{39}K-rates in 100 s [$R_{AMS}(^{39}K)$], as well as the $^{127}I^-$ or $^{63}Cu^-$ beam currents at the LECup [$I_{LE}{}^{127}I^-/{}^{63}Cu^-$)], corresponding to the CsI and organic-sample runs, respectively. The quoted ^{39}K-levels were derived from the means of those 10 measurements from 600 to 1600 s. Typical statistical errors of individual measurement is less than 1%, while the variance of the 10 measurements are of the order of 10%. The variances include systematic effects like unstable hardware conditions during data taking, and are adopted as the measurement uncertainties.

Table 2
Beam currents and transmission efficiencies of the negative ^{37}Cl ions

Measuring cup	Beam current (nA)	Transmission efficiency	
		This stage	Cumulative
Low energy cup	900	1.00	1.00
Image cup	350	0.39	0.39
AMS cup	150	0.43	0.17

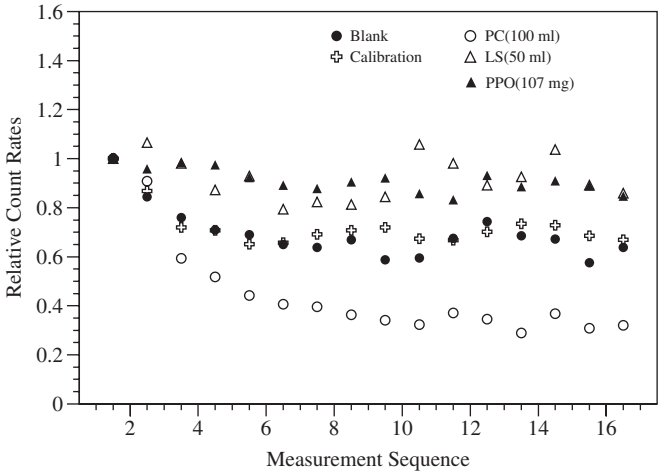

Fig. 3. Time evolution of the ^{39}K-rates for some selected samples. Results after the sixth measurements since the start of data taking were adopted for subsequent analysis.

The background-subtracted rates in 100 s at the normalized currents of $I_{LE} = 1000$ nA, denoted by $N_{AMS}(^{39}K)$, are given by

$$N_{\text{AMS}}(^{39}\text{K}) = R_{\text{AMS}}(^{39}\text{K}) \cdot \frac{1000\,\text{nA}}{I_{\text{LE}}} - N^0_{\text{AMS}}(^{39}\text{K}) \tag{5}$$

where the superscript "0" represents the background values under the same normalizations. The ^{39}K-contaminations in the samples can then be derived from $N_{AMS}(^{39}K)$, via comparisons with reference samples with known ^{39}K concentrations.

There are inevitable variations in the potassium contaminations among different batches of the same sample category. As an illustrative example, a recent study [21] showed the ^{40}K activities varied by a factor of five among building materials. Accordingly, the AMS measurements discussed here would have ~10% uncertainties for those particular samples being measured, but would just imply the order of magnitude contamination levels expected on the generic sample categories.

3.1. Blind target

In a typical AMS measurement, the samples are placed inside a 1 mm diameter hole drilled out of a target structure made of electrolytic aluminium. The sputtering ions are then focused on to this hole.

Measurements were performed with "blind" targets where the target structure was replaced by a piece of solid metal. This allowed measurements of the intrinsic background due to ambient contaminations and accelerator operation. Three target materials were selected: ultra-pure (<ppm) copper, electrolytic copper and electrolytic aluminium. Displayed in Fig. 4 are the time-variations of

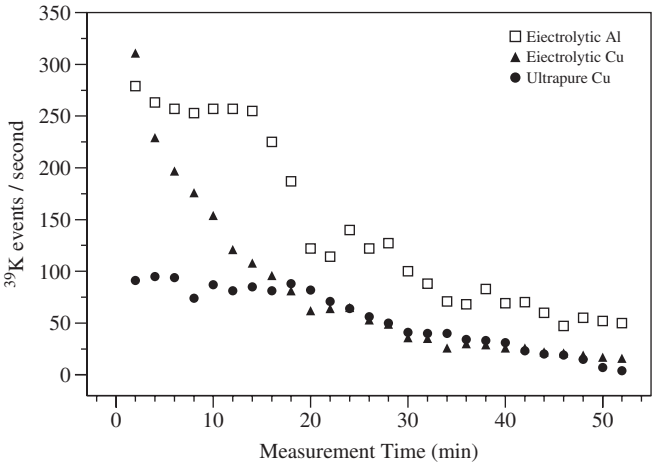

Fig. 4. Time evolution of the ^{39}K-rates for the blind target runs under the same hardware operating conditions as those for the sample measurements.

their ^{39}K background at the AMS detector under the same hardware operating conditions as those for the measurements with samples. The initial enhancement of background is due to surface contaminations of the target materials not relevant to subsequent studies, while the steady-state rates represent the upper bounds of the ion beam and accelerator background. The steady levels of $\sim$50 ^{39}K-events per second for the aluminium target are at least factors of 20 less than the typical rates in the measurements of various samples ($>1000\,s^{-1}$) such that the accelerator-related background can be neglected at the expected $\sim$10% accuracy level discussed in this article.

3.2. Inorganic CsI powder

The contaminations of ^{39}K in CsI were directly measured by counting methods with the AMS detector, using KI as the reference sample. The two measurements on CsI and KI were normalized by the LECup currents $I_{LE}(^{127}I^-) = 1000\,nA$. The ^{39}K-contents in KI were measured as beam currents in the Image Cup [$I_{Im}(^{39}K^{8+})$], and converted to an equivalent normalized ^{39}K-rates at the AMS detector, via

$$N_{KI}(^{39}K) = \varepsilon_{Im\to AMS}\cdot\left[\frac{I_{Im}(^{39}K^{8+})/\mu A}{1.6\times10^{-13}}\right]\cdot\left[\frac{1000\,nA}{I_{LE}(^{127}I^-)}\right] \quad (6)$$

where $\varepsilon_{Im\to AMS} = 43\%$ is the measured transmission efficiency between the Image Cup and the AMS detector from Table 2. The calibration relation for the CsI measurements can therefore be given as

$$[^{39}K/CsI] = [^{39}K/KI]\cdot\frac{M(KI)}{M(CsI)}\cdot\frac{N_{AMS}(^{39}K)}{N_{KI}(^{39}K)}. \quad (7)$$

The evaluation of the normalized ^{39}K-rates [$N_{AMS}(^{39}K)$] follows from Eq. (5), where the measured raw rate was $R_{AMS}(^{39}K) = (415\,000\pm25\,000)/(100\,s)$ at $I_{LE}(^{127}I^-) = 3510\,nA$. The ^{39}K background in the CsI measurements are due the ion beams and accelerator. As discussed in Section 3.1, the range of $N^0_{AMS}(^{39}K)\sim O(10)\,s^{-1}$ is negligible compared to the potassium contamination levels in the CsI samples.

Applying the formulae, the measured contamination levels of potassium in CsI are:

$$[^{39}K/CsI] = (5.2\pm1.3)\times10^{-7}\,g/g$$

or equivalently

$$[^{40}K/CsI] = (6.5\pm1.6)\times10^{-11}\,g/g. \quad (8)$$

This implies an activity ^{40}K decays in CsI of $(1440\pm360)\,kg^{-1}\,day^{-1}$. This result is consistent with and improves over that of an independent measurement on the CsI powder by direct counting of the 1461 keV photons with an HPGe detector, where only an upper limit

$$[^{40}K/CsI] < 2\times10^{-10}\,g/g \quad (9)$$

could be derived.

As an illustrative comparison, the intrinsic contaminations of ^{137}Cs and the U + Th series in CsI(Tl) crystals were recently studied [22], where the levels of

$$[^{137}Cs/CsI(Tl)] = (1.7\pm0.3)\times10^{-17}\,g/g$$
$$[^{232}Th/CsI(Tl)] = (2.23\pm0.06)\times10^{-12}\,g/g$$
$$[^{238}U/CsI(Tl)] = (8.2\pm0.2)\times10^{-13}\,g/g$$

and

$$[^{235}U/CsI(Tl)] < 4.9\times10^{-13}\,g/g \quad (10)$$

were derived. These results confirm the expectations that the potassium contaminations in most materials are usually higher than those of the other isotopes which also exist in abundance in nature.

3.3. Organic solid and liquid

The results of the various runs with different organic samples are summarized in Table 3. As discussed in Section 2.1 and illustrated in Fig. 2, the chemical preprocessing of the samples turned them into solid powder mixtures of $CuO + KNO_3$. Consequently, the AMS measurements of the ^{39}K levels in the samples were all made relative to ^{63}Cu. The time evolution of the 16 measurements for some selected samples are displayed in Fig. 3 as illustrations.

All the 13 measurements listed in Table 3 were performed within 12 h where the accelerator operation has been stable. The calibration samples with known [^{39}K/Cu] contamination levels served to establish a relationship between the ^{39}K-rates and $^{63}Cu^-$ beam currents. The good agreement of the cross-check samples with expected results, as well as the internal consistencies of the measured [^{39}K/sample] levels among the different categories of samples, demonstrate that the experimental conditions were constant throughout the measurements, and that a single calibration relation can be applied consistently to all data.

Table 3
Summary of the results of the various AMS measurements with different configurations

Samples	[^{39}K/Cu] (g/g)	[^{39}K/sample] (g/g)	[^{40}K/sample (g/g)
Blank			
No sample	$(1.6 \pm 0.1) \times 10^{-8}$	–	–
Calibration			
[^{39}K/Cu]= 1.5e − 7 g/g	–	–	–
Cross-checks			
[^{39}K/Cu]= 1.5e − 8 g/g	$(1.7 \pm 0.2) \times 10^{-8}$	–	–
[^{39}K/Cu]= 1.5e − 9 g/g	$(2.4 \pm 2.0) \times 10^{-9}$	–	–
PPO Powder			
Mass = 1.8 mg	$(9.5 \pm 0.7) \times 10^{-8}$	$(5.3 \pm 0.4) \times 10^{-7}$	$(6.6 \pm 0.5) \times 10^{-11}$
Mass = 19 mg	$(9.8 \pm 1.0) \times 10^{-7}$	$(5.2 \pm 0.5) \times 10^{-7}$	$(6.5 \pm 0.7) \times 10^{-11}$
Mass = 107 mg	$(5.8 \pm 0.2) \times 10^{-6}$	$(5.4 \pm 0.2) \times 10^{-7}$	$(6.8 \pm 0.3) \times 10^{-11}$
Pseudocumene			
Volume = 1 ml	$(-3 \pm 13) \times 10^{-10}$	$<2.2 \times 10^{-11}$	$<2.8 \times 10^{-15}$
Volume = 5 ml	$(7 \pm 27) \times 10^{-10}$	$<1.2 \times 10^{-11}$	$<1.5 \times 10^{-15}$
Volume = 100 ml	$(9.3 \pm 1.0) \times 10^{-8}$	$(1.1 \pm 0.1) \times 10^{-11}$	$(1.4 \pm 0.1) \times 10^{-15}$
Liquid scintillator (commercial)			
Volume = 1 ml	$(9.6 \pm 0.5) \times 10^{-8}$	$(1.10 \pm 0.06) \times 10^{-9}$	$(1.38 \pm 0.07) \times 10^{-13}$
Volume = 5 ml	$(4.4 \pm 0.2) \times 10^{-7}$	$(1.01 \pm 0.04) \times 10^{-9}$	$(1.27 \pm 0.06) \times 10^{-13}$
Volume = 50 ml	$(4.3 \pm 0.4) \times 10^{-6}$	$(1.0 \pm 0.1) \times 10^{-9}$	$(1.3 \pm 0.1) \times 10^{-13}$

The two measurements with small volume of pseudocumene did not give statistically significant results so that only 90% confidence level limits are quoted.

The details of the measurements are elaborated in the following subsections.

3.3.1. Blank (Sample-less) Measurement

A measurement was performed where the exact procedures of Fig. 2 as described in Section 2.1 were followed—except that there were no initial samples. This allows the studies of the intrinsic ^{39}K background due to the chemical processing procedures.

The measured background was $R^0_{\mathrm{AMS}}(^{39}\mathrm{K}) = (73600 \pm 5600)/(100\,\mathrm{s})$ at a beam current of $I^0_{\mathrm{LE}}(^{63}\mathrm{Cu}^-) = 778\,\mathrm{nA}$, or equivalently

$$N^0_{\mathrm{AMS}}(^{39}\mathrm{K}) = (94\,600 \pm 7200)/(100\,\mathrm{s}). \quad (11)$$

This background was subtracted off from the various AMS measurements on organic samples, from which their intrinsic ^{39}K-contaminations were derived. Using the calibration relation derived in Section 3.3.2, this corresponds to a background level of

$$[^{39}\mathrm{K}/\mathrm{Cu}]_{\mathrm{Bkg}} = (1.62 \pm 0.12) \times 10^{-8}\,\mathrm{g/g}. \quad (12)$$

As discussed in Section 3.1, the beam-related background from the blind target measurement was only of the order of ~50 ^{39}K events per second. Accordingly, the measured ^{39}K background of Eq. (12) is expected to be introduced pre-dominantly in the processing procedures.

3.3.2. Reference samples

A series of potassium–copper standard samples were prepared. The copper[6] was of ultra-pure grade, with purity level better than ppm and potassium contaminations less than 10 ppb. Added to it were 65% ultra-pure nitric acid and 99.99% potassium nitrate (KNO_3). The ^{39}K levels were independently verified by spark source mass spectrometry [5]. The exact processing procedures of Fig. 2 were followed.

The sample with highest potassium concentration, at $[^{39}\mathrm{K}/\mathrm{Cu}] = 1.50 \times 10^{-7}\,\mathrm{g/g}$, was used for calibration purposes. The measurements were $R_{\mathrm{AMS}}(^{39}\mathrm{K}) = (557\,000 \pm 19\,000)/(100\,\mathrm{s})$ at $I_{\mathrm{LE}}(^{63}\mathrm{Cu}^-) = 550\,\mathrm{nA}$, corresponding to $N_{\mathrm{AMS}}(^{39}\mathrm{K}) = (1.01 \pm 0.03) \times 10^6/(100\,\mathrm{s})$ after background subtraction and beam current normalization. The overall calibration relation for subsequent measurements is therefore:

$$[^{39}\mathrm{K}/\mathrm{Cu}] = 1.5 \times 10^{-7} \cdot \frac{N_{\mathrm{AMS}}(^{39}\mathrm{K})}{1.01 \times 10^6}\,\mathrm{g/g} \quad (13)$$

where $N_{\mathrm{AMS}}(^{39}\mathrm{K})$ can be evaluated using Eq. (5). This relation was applied consistently to all other samples listed in Table 3.

Two additional samples with 10 and 100 times lower potassium concentrations were prepared to cross-check the procedures. The AMS measurement results, shown in Table 3, were derived after applying this conversion factor and subtracting the normalized background. They are in excellent agreement with the expected values.

The ^{39}K-levels in [^{39}K/sample] units for the subsequent samples can be derived through

$$[^{39}\mathrm{K}/\mathrm{sample}] = [^{39}\mathrm{K}/\mathrm{Cu}] \cdot \left[\frac{M(\mathrm{Cu})}{M(\mathrm{sample})}\right] \quad (14)$$

where M(Cu) and M(sample) are the controlled and known masses of copper and the sample, respectively. It can be seen that given a sample with definite [^{39}K/sample],

[6]Supplier: Alfa Aesar, USA.

the uncertainties in the measurement of [^{39}K/Cu] can be reduced by using larger sample mass for the same amount of copper carrier introduced. The final results in [^{40}K/sample] follow simply from taking ratios on the isotopic abundance between ^{40}K and ^{39}K.

3.3.3. PPO concentration scan

The relation established in Eq. (13) is applicable for AMS measurements in solid samples following the processing procedures of Fig. 2. For organic liquid samples, an extra factor—the survival efficiency of potassium at the solid residuals after vacuum evaporation (ε)—has to be evaluated. This was studied by measuring the ^{39}K-yields in solid PPO (Y_{PPO}) and comparing it to those samples with PPO mixed with PC. The efficiency ε is given by

$$\varepsilon = \frac{Y_\alpha - Y_0}{\alpha \cdot Y_{\mathrm{PPO}}} \tag{15}$$

where Y_{PPO}, Y_0, and Y_α are, respectively, the ^{39}K-levels in PPO solid, pure PC liquid without PPO and PC mixed with PPO in known fractions α. The results are summarized in Table 4. The most accurate measurement is one with a high concentration of PPO ($\alpha = 1\%$), giving $\varepsilon = (1.0 \pm 0.1)$. This result demonstrates that most potassium in the PPO + PC solution remained in the solid residuals after evaporation. Measurements with lower PPO concentrations were still consistent with complete potassium extraction, but with larger uncertainties due to limited statistics above the background.

3.3.4. LS, Solute and Solvent

Samples of different masses of pure PPO powder, pure PC liquid, as well as their mixtures as LSs were measured, using the background subtraction procedures and calibration relation discussed above. The results are summarized in Table 3. Consistent results were obtained for the two decades variations in sampling mass.

The LS sample was commercially mixed. The measured ^{40}K contamination was

$$[^{40}\mathrm{K}/\mathrm{LS}] = (1.3 \pm 0.1) \times 10^{-13}\,\mathrm{g/g} \tag{16}$$

implying equivalently a ^{40}K-activity of $\sim 3\,\mathrm{kg}^{-1}\,\mathrm{day}^{-1}$. Such commercial LS sample is not yet good enough for the low-background experiments. Further purifications are therefore necessary. The source of contaminations comes primarily from the PPO solute, such that it would be more effective to focus the purification program on it. The best measurement is, expectedly, one on pure PC at the largest sampling mass, where

$$[^{40}\mathrm{K}/\mathrm{PC}] = (1.4 \pm 0.1) \times 10^{-15}\,\mathrm{g/g}. \tag{17}$$

The expected ^{40}K-decay rate is $(0.024 \pm 0.003)\,\mathrm{kg}^{-1}\,\mathrm{day}^{-1}$. These characteristic features should be valid in general—that the contaminations in organic LS come primarily from the dye solutes while the liquid solvents are orders of magnitude cleaner. Another two measurements of PC with much smaller sampling masses did not give rise to statistically significant excess of the [$_{39}$K/Cu] ratio, such that only 90% confidence level upper limits are derived [6] in Table 3. The limits are consistent with the measured results of Eq. (17).

It is instructive to compare the results of Tables 3 and 4, which are from the measurements on two different batches of PPO and PC samples from the same supplier. The ^{39}K contaminations of the two batches of PPO are, respectively, $Y_{\mathrm{PPO}} = (5.4 \pm 0.2) \times 10^{-7}$ and $(3.1 \pm 0.4) \times 10^{-8}$ g/g, while the those for the PC are $Y_0 = (1.1 \pm 0.1) \times 10^{-11}$ and $(1.5 \pm 0.2) \times 10^{-11}$ g/g. The differences indicate the range of variations of potassium levels in different production batches among the same materials.

Table 4
Results from AMS measurements with varying PPO concentration in PC

Samples	α (%)	[^{39}K/sample] (g/g)	ε
PPO solid	100	$Y_{\mathrm{PPO}} = (3.1 \pm 0.4) \times 10^{-8}$	–
Pure PC	0.0	$Y_0 = (1.5 \pm 0.2) \times 10^{-11}$	–
PC + PPO	0.01	$Y_\alpha = (1.8 \pm 0.3) \times 10^{-11}$	1.0 ± 1.3
PC + PPO	0.1	$Y_\alpha = (4.4 \pm 0.8) \times 10^{-11}$	1.0 ± 0.3
PC + PPO	1.0%	$Y_\alpha = (3.2 \pm 0.1) \times 10^{-10}$	1.0 ± 0.1

3.4. Limiting sensitivities

An important parameter to characterize the performance of this measurement technique is the limiting sensitivity. It represents the upper limits that can be set for samples where no excess of ^{39}K-rates above background are observed—or alternatively, the minimal contamination levels that will produce a positive measurement.

The measurements of the CsI samples do not involve chemical pre-processing. Therefore, the sensitivity is limited by the uncertainties to the ion-beam related background measured in the "blind target" run discussed in Section 3.1. A measurement with 10% accuracy on the ^{39}K-background count rates for the copper target implies an uncertainty of $<3\,\mathrm{s}^{-1}$ at the AMS detector. This can be translated to limiting sensitivities following the calibration relation of Eq. (7):

$$[^{39}\mathrm{K}/\mathrm{CsI}]_{\mathrm{limit}} \sim 4 \times 10^{-10}\,\mathrm{g/g}, \text{ or equivalently}$$
$$[^{40}\mathrm{K}/\mathrm{CsI}]_{\mathrm{limit}} \sim 5 \times 10^{-14}\,\mathrm{g/g}. \tag{18}$$

For organic liquid, potassium introduced during the pre-processing procedures is the dominant background. The limiting sensitivities of [^{39}K/Cu] can be derived from the uncertainties of the background blank measurement in Eq. (12), giving

$$[^{39}\mathrm{K}/\mathrm{Cu}]_{\mathrm{limit}} \sim 2 \times 10^{-9}\,\mathrm{g/g}. \tag{19}$$

To convert into [^{39}K/(Org.Liq.)] units, the relation of Eq. (13) is used. The ratio of [M(sample)/M(Cu)] is taken from the measurement with the largest liquid sample volume (100 ml) where the extraction of the contaminants

was successfully demonstrated. The sensitivities are

$$[^{39}\mathrm{K}/(\mathrm{Org.Liq.})]_{\mathrm{limit}} \sim 2 \times 10^{-13}\ \mathrm{g/g}$$

or equivalently

$$[^{40}\mathrm{K}/(\mathrm{Org.Liq.})]_{\mathrm{limit}} \sim 3 \times 10^{-17}\ \mathrm{g/g}. \quad (20)$$

The improvement of sensitivities in Eqs. (18) and (20) of organic liquid over solid CsI powder can be readily understood in terms of the evaporation and extraction processes for the liquids. The chemistry treatment introduces potassium background which reduces the sensitivities by a factor of 10. This is compensated by a large $[M(\mathrm{Cu})/M(\mathrm{sample})]$ ratio following the conversion relation of Eq. (14). At a typical $M(\mathrm{Cu}) \sim 10$ mg and the largest liquid extraction volume of 100 ml [that is, $M(\mathrm{sample}) \sim 100$ g], a sensitivity enhancement of 10^{-4} is readily attained.

4. Summary and outlook

In this article, we report the first measurement of ultra-low potassium contaminations in an inorganic salt (CsI) and in an organic LS (LS = PC + PPO) using AMS. Comparable sensitivities to the neutron activation techniques were achieved. Potassium were positively identified in samples of commercially available CsI and LS, at the contamination levels of 7×10^{-11} and 1.3×10^{-13} g/g, respectively. The radioactivity in the LS is mainly due to the dye solutes. The limiting sensitivities of the techniques are of the order of 10^{-14} g/g of ^{40}K in solid powder and of 10^{-17} g/g of ^{40}K in an organic liquid.

The raw AMS measurements of Eqs. (8) and (12) give $[^{39}\mathrm{K}/\mathrm{CsI}]$ and $[^{39}\mathrm{K}/\mathrm{Cu}]$ to be at the range of $10^{-7}-10^{-8}$ g/g. This is much higher than the intrinsic AMS sensitivity ranges for the other isotopes ($<10^{-12}$ g/g). Consequently, background due to other $A = 39$ isotopes or residual molecular interference is expected to be negligible. The observed counts in the AMS measurements were indeed due to the detection of ^{39}K ions. The limiting sensitivities of Section 3.4 are constrained by the presence of ambient potassium impurities in the system.

In the case of organic liquid, the potassium was introduced during the chemical processing of the liquid depicted in Fig. 2. Further improvement can be made along these directions. The beam-related background is low in comparison. A boost in sensitivities can also be made with the use of larger initial liquid volume for evaporation. The largest sample demonstrated in the present studies is 100 ml. Extensions to treatment of liter-scale sample are technically similar—and have been demonstrated for samples up to 600 ml in Ref. [15]. Therefore, a limiting sensitivity of $\sim 10^{-18}$ g/g on organic liquid using AMS should be possible and realistic.

This work demonstrates the feasibilities of measuring ultra-low impurities of naturally occurring yet unstable isotopes with AMS. Accordingly, other radio-isotopes which are problematic to low-background experiments, such as the ^{238}U and ^{238}Th series as well as ^{87}Rb, ^{113}Cd, ^{115}In, ^{138}La and ^{176}Lu, can also be measured by the AMS techniques. The goals of our future efforts would be to devise schemes to measure some of these isotopes. Extensions to Rb will be relatively straightforward, while the measurements of the ^{238}U and ^{238}Th series will involve upgrades of the present accelerator systems.

Acknowledgments

The authors are grateful to M. Lin, S.H. Li, Y.D. Chen, A.L. Li, J. Li, K.X. Liu, B.F. Ni, H.Q. Tang, W.Z. Tian and Z.Y. Zhou for helpful discussions, as well as to Q.B. You, Y.W. Bao, Y.M. Hu and the technical staff at CIAE for smooth accelerator operation. This work is supported by Contracts 10375099 from the National Natural Science Foundation, China, and 95-2119-M-001-028 from the National Science Council, Taiwan.

References

[1] C. Tuniz, et al., Accelerator Mass Spectrometry, CRC Press, Boca Raton, FL, 1998.
[2] D. Elmore, F.M. Phillips, Science 346 (1987) 543.
[3] C. Tuniz, Radiat. Phys. Chem. 61 (2001) 317.
[4] Y.F. Liu, et al., Pure Appl. Chem. 66 (1994) 305.
[5] J.S. Becker, H.-J. Dietze, Spectrochim. Acta B 1475 (1998).
[6] See the respective sections in Review of Particle Physics, J. Phys. G 33 (2006) 1 for details and references.
[7] H.T. Wong, Mod. Phys. Lett. A 19 (2004) 1207.
[8] K.J. Dong, et al., Nucl. Instr. and Meth. B 259 (2007) 271.
[9] C. Arpesella, et al., Astroparticle Phys. 18 (2002) 1.
[10] K. Eguchi, et al., Phys. Rev. Lett. 90 (2003) 021802.
[11] W.R. Smythe, Phys. Rev. 35 (1939) 316;
A.K. Brewer, Phys. Rev. 55 (1939) 669.
[12] G. Heusser, Nucl. Instr. and Meth. B 58 (1991) 79;
P. Jagam, J.J. Simpson, Nucl. Instr. and Meth. A 324 (1993) 389.
[13] G. Alimonti, et al., Nucl. Instr. and Meth. A 406 (1998) 411.
[14] R.V. Hentig, et al., Fres. J. Anal. Chem. 360 (1998) 664.
[15] Z. Djurcic, et al., Nucl. Instr. and Meth. A 507 (2003) 680.
[16] U. Fehn, et al., Nature 323 (1986) 707;
J.C. Rucklidge, G.C. Wilson, L.R. Kilius, Nucl. Instr. and Meth. B 52 (1990) 507;
H.E. Gove, et al., Nucl. Instr. and Meth. B 52 (1990) 502.
[17] F.D. McDaniel, et al., Nucl. Instr. and Meth. B 190 (2002) 826;
L.J. Mitchell, et al., Nucl. Instr. and Meth. B 219 (2004) 455.
[18] S. Jiang, et al., Nucl. Instr. and Meth. B 52 (1990) 285;
S. Jiang, et al., Nucl. Instr. and Meth. B 92 (1994) 61.
[19] H.B. Li, et al., Nucl. Instr. and Meth. A 459 (2001) 93;
Y. Liu, et al., Nucl. Instr. and Meth. A 482 (2002) 125.
[20] H. Park, et al., Nucl. Instr. and Meth. A 491 (2002) 460;
T.Y. Kim, et al., Nucl. Instr. and Meth. A 500 (2003) 337.
[21] A. Kumar, et al., Radiat. Meas. 36 (2003) 465.
[22] Y.F. Zhu, et al., Nucl. Instr. and Meth. A 557 (2006) 490.